Multiphysics Optimization of an Aircraft Winglet via CFD–FEM Coupling and Radial Basis Function Mesh Morphing

Marco Evangelos Biancolini

University of Rome Tor Vergata

Introduction

- Fluid-Structure Interaction (FSI), in most engineering applications, cannot be neglected.
- CFD analysts → boundaries rigid, verification of the aeroelastic performance to a post design phase
- Structural analysts → fluid as constant pressure on the walls
- Several techniques in literature, each one with pros and cons
- Mesh morphing technologies, missing link between CFD and CSM

Modal superposition: overview

- Structural modes, and related frequency signature, represent the basic nature of the **dynamic behaviour** of a structure
- FSI with modal approach: **simplified environment** for static and dynamic aeroelastic mechanisms

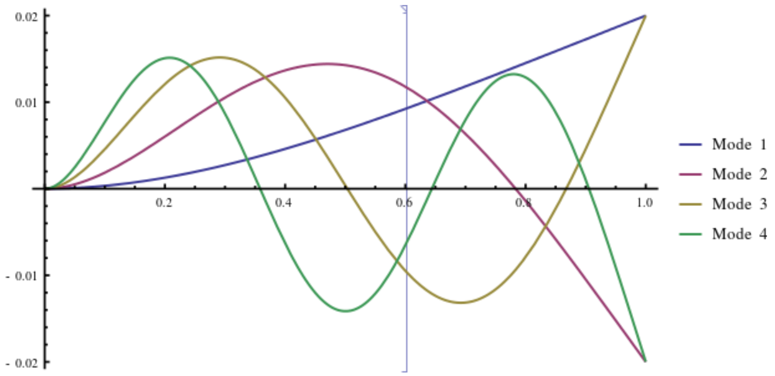

- Limited to **linear** structural problems
- CFD is made flexible importing modes and frequencies, NO data exchange
- CFD mesh deformation required: RBF Mesh morphing

Radial Basis Functions

- RBF are at the core of the RBF Morph software family, integrated in ANSYS Workbench, Fluent and available as a Standalone
- RBFs are a mathematical tool capable to **interpolate** at a generic point in the space a function **known** in a discrete set of points (**source points**)

$$s(\boldsymbol{x}) = \sum_{i=1}^{N} \overbrace{\gamma_i \varphi\left(\underbrace{\left\| \boldsymbol{x} - \boldsymbol{x}_{k_i} \right\|}_{\text{distance from the i-th source point}}\right)}^{\text{radial basis}} + \overbrace{h(\boldsymbol{x})}^{\text{polynomial}}$$

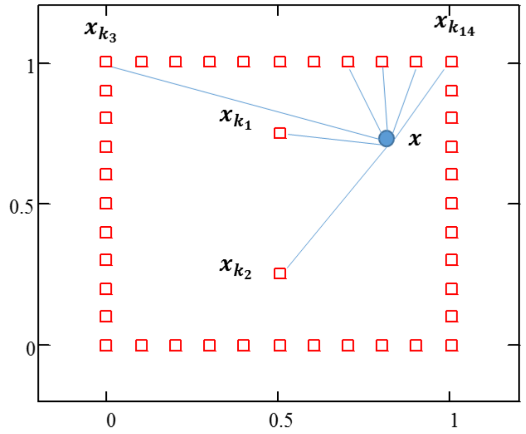

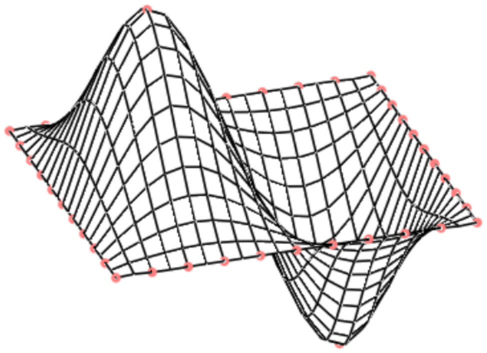

Radial Basis Functions

- If evaluated at the source points, the interpolating function gives exactly the input values:

$$s(\boldsymbol{x}_{k_i}) = g_i \qquad h(\boldsymbol{x}_{k_i}) = 0 \qquad 1 \le i \le N$$

- The RBF problem is associated to the solution of the linear system:

$$\begin{bmatrix} \mathbf{M} & \mathbf{P} \\ \mathbf{P}^{\mathrm{T}} & 0 \end{bmatrix} \begin{pmatrix} \boldsymbol{\gamma} \\ \boldsymbol{\beta} \end{pmatrix} = \begin{pmatrix} \boldsymbol{g} \\ 0 \end{pmatrix} \qquad M_{ij} = \varphi\left(\boldsymbol{x}_{k_i} - \boldsymbol{x}_{k_j} \right) \qquad 1 \le i, j \le N \qquad \mathbf{P} = \begin{bmatrix} 1 & x_{k_1} & y_{k_1} & z_{k_1} \\ 1 & x_{k_2} & y_{k_2} & z_{k_2} \\ \vdots & \vdots & \vdots & \vdots \\ 1 & x_{k_N} & y_{k_N} & z_{k_N} \end{bmatrix}$$

Radial Basis Functions

- Once solved the RBF problem, each displacement component is interpolated:

$$\begin{cases} s_x(\boldsymbol{x}) = \sum_{i=1}^{N} \gamma_i^x \varphi\left(\boldsymbol{x} - \boldsymbol{x}_{k_i}\right) + \beta_1^x + \beta_2^x x + \beta_3^x y + \beta_4^x z \\ s_y(\boldsymbol{x}) = \sum_{i=1}^{N} \gamma_i^y \varphi\left(\boldsymbol{x} - \boldsymbol{x}_{k_i}\right) + \beta_1^y + \beta_2^y x + \beta_3^y y + \beta_4^y z \\ s_z(\boldsymbol{x}) = \sum_{i=1}^{N} \gamma_i^z \varphi\left(\boldsymbol{x} - \boldsymbol{x}_{k_i}\right) + \beta_1^z + \beta_2^z x + \beta_3^z y + \beta_4^z z \end{cases}$$

RBF	φ(r)	RBF	φ(r)
Spline type (Rn)	r^n, n odd	Inverse multiquadratic (IMQ)	$\frac{1}{\sqrt{1+r^2}}$
Thin plate spline	$r^n \log(r)$ n even	Inverse quadratic (IQ)	$\frac{1}{1+r^2}$
Multiquadratic (MQ)	$\sqrt{1+r^2}$	Gaussian (GS)	e^{-r^2}

Parametric mesh formulation

- Each node position of the volume mesh can be computed using its original position as input:

$$\boldsymbol{x}_{\boldsymbol{node}_{\boldsymbol{new}}} = \boldsymbol{x}_{\boldsymbol{node}} + \begin{bmatrix} s_x(\boldsymbol{x}_{\boldsymbol{node}}) \\ s_y(\boldsymbol{x}_{\boldsymbol{node}}) \\ s_z(\boldsymbol{x}_{\boldsymbol{node}}) \end{bmatrix}$$

- Modal theory is linear, no need to use the costly RBF formula each mesh update. The following linear combination is used:

$$\boldsymbol{X}_{\boldsymbol{CFD}} = \boldsymbol{X}_{\boldsymbol{CFD}_0} + \sum_{m=1}^{n} \eta_m \, \boldsymbol{\Delta u}_m$$

Modal superposition – static FSI

- Modes and frequencies of a structure can be obtained solving the eigenvalue problem:

$$\boldsymbol{K}\boldsymbol{u} = \omega^2 \boldsymbol{M}\boldsymbol{u}$$

- Orthogonality of modes and low pass behaviour simplify the problem. Mass normalization further simplifies the framework:

$$\boldsymbol{\Delta u}_m^T \boldsymbol{M} \boldsymbol{\Delta u}_m = 1 \qquad \boldsymbol{\Delta u}_m^T \boldsymbol{K} \boldsymbol{\Delta u}_m = \omega_m^2 \qquad \boldsymbol{u} = \sum_{m=1}^{n} \boldsymbol{\Delta u}_m \, \eta_m = \boldsymbol{\Delta u} \, \boldsymbol{\eta}$$

$$\ddot{\eta}_m + {\omega_m}^2 \eta_m = F_m \qquad m = 1,2, \dots, n \qquad {\omega_m}^2 \eta_m = F_m$$

Modal superposition – unsteady FSI

- Equation of motion can be employed with finite differences
- Duhamel integral can be used to calculate modal coordinates

$$\eta(t) = e^{-\varsigma\omega_n t}\left[\eta_0 \cos(\omega_d t) + \frac{\dot{\eta}_0 + \varsigma\omega_n\eta_0}{\omega_d}\sin(\omega_d t)\right] + e^{-\varsigma\omega_n t}\left\{\frac{1}{m\omega_d}\int_0^t e^{-\frac{b(t-\tau)}{2m}} f(\tau)\sin[\omega_d(t-\tau)]dx\right\}$$

- For a generic numerical analysis, if the load is constant for each timestep, the Duhamel integral can be written as:

$$\omega_d = \omega_n\sqrt{1-\varsigma^2}$$

$$\eta(t+\Delta t) = e^{-\varsigma\omega_n\Delta t}\left[\eta(t)\cos(\omega_d\Delta t) + \frac{\dot{\eta}(t) + \varsigma\omega_n\eta(t)}{\omega_d}\sin(\omega_d\Delta t)\right] + e^{-\varsigma\omega_n\Delta t}\left\{\frac{F(t)}{\omega_d}\left[\frac{4\omega_d}{\varsigma^2\omega_n^2 + 4\omega_d^2} - e^{-\varsigma\omega_n\Delta t}\frac{2\varsigma\omega_n\sin(\omega_d\Delta t) + 4\omega_d\cos(\omega_d\Delta t)}{\varsigma^2\omega_n^2 + 4\omega_d^2}\right]\right\}$$

Modal superposition workflow

- No interpolation required, no data exchange required, modes are embedded as pre-processing
- Steady / unsteady FSI, FSI with prescribed motion
- How many modes to employ? Modal truncation error: modal basis qualification

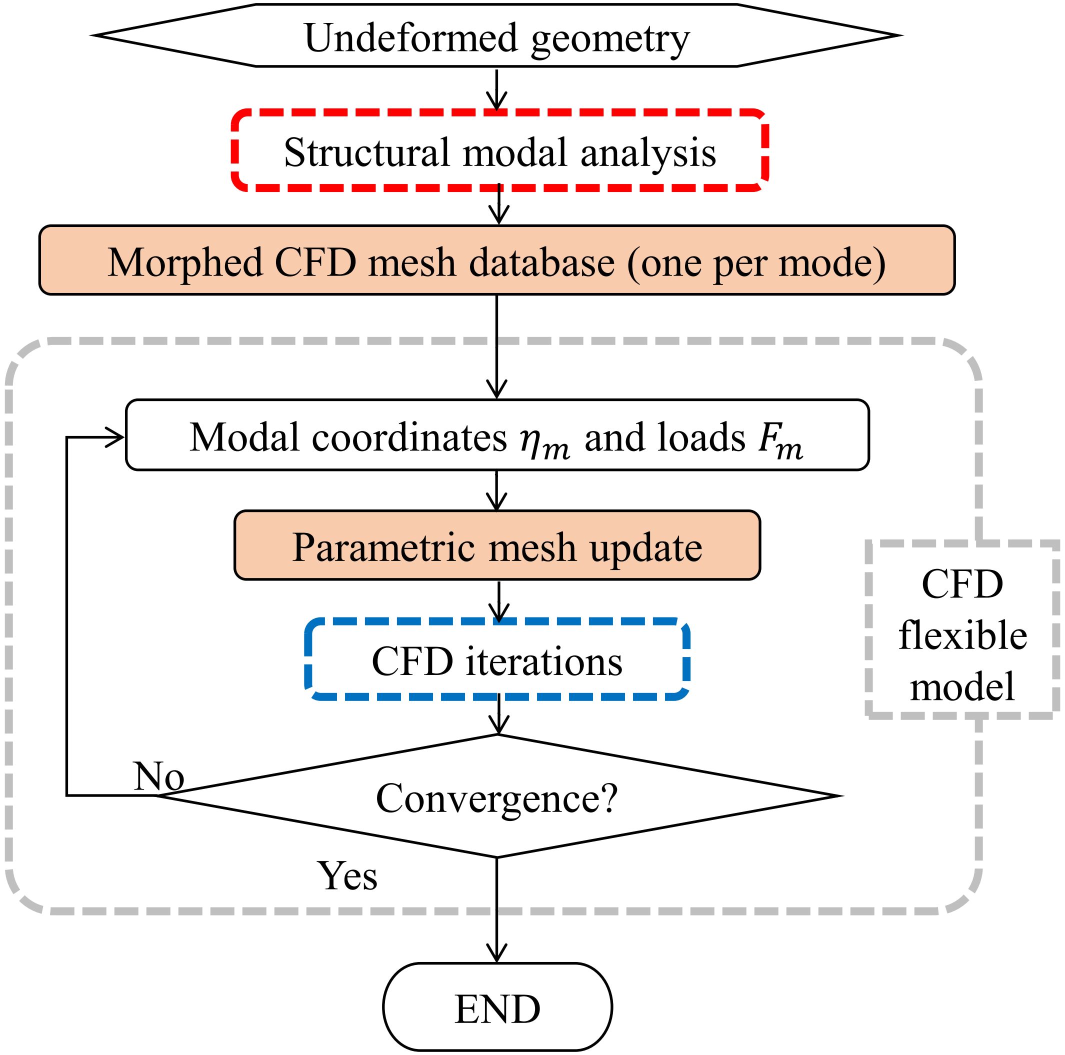

Steady business-jet aircraft

- Piaggio Aerospace business-jet aircraft, P1XX

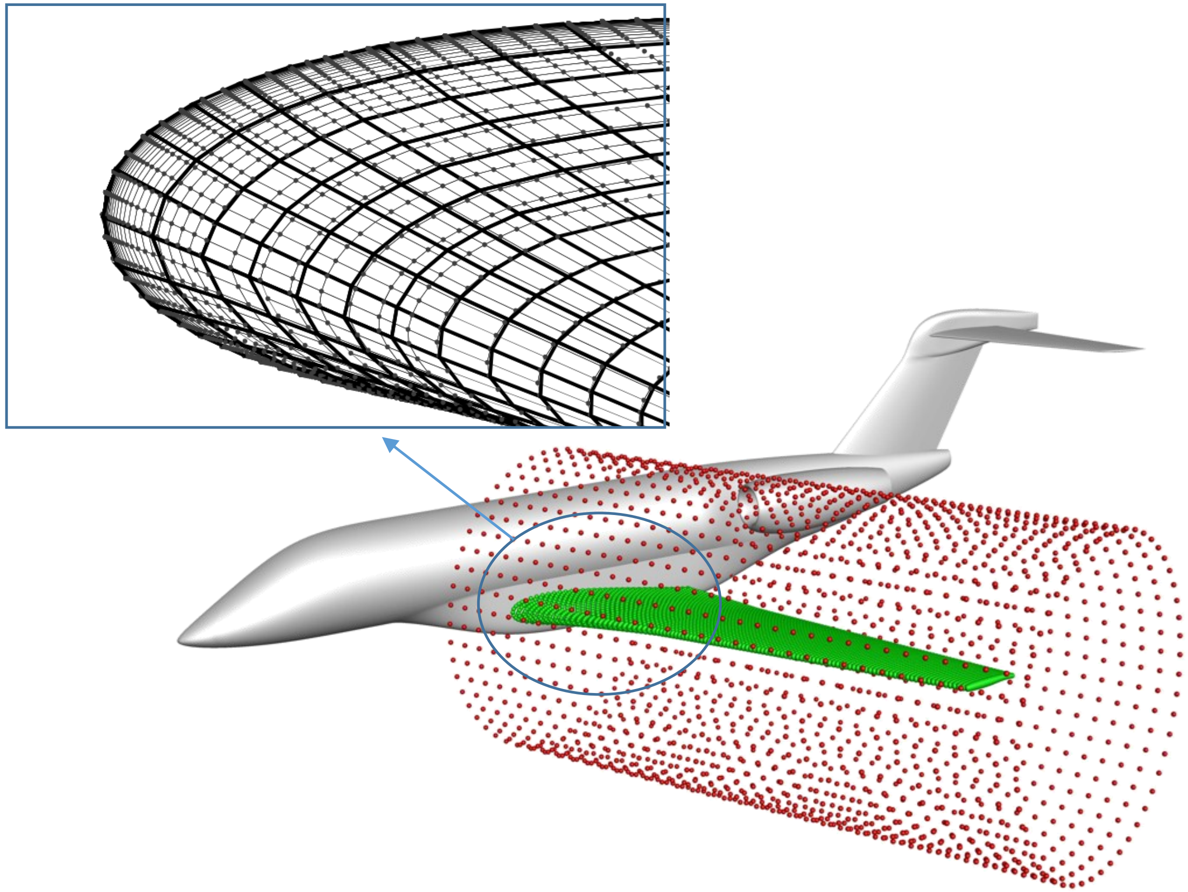

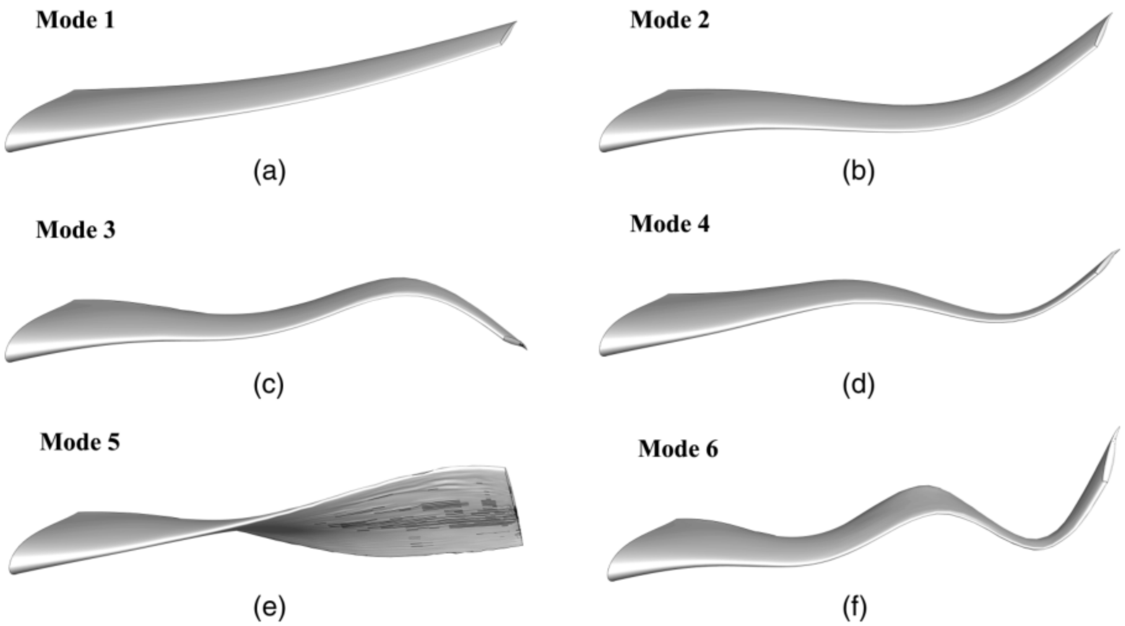

Steady business-jet aircraft

- Good match with 2-way FSI, few iterations, few modes

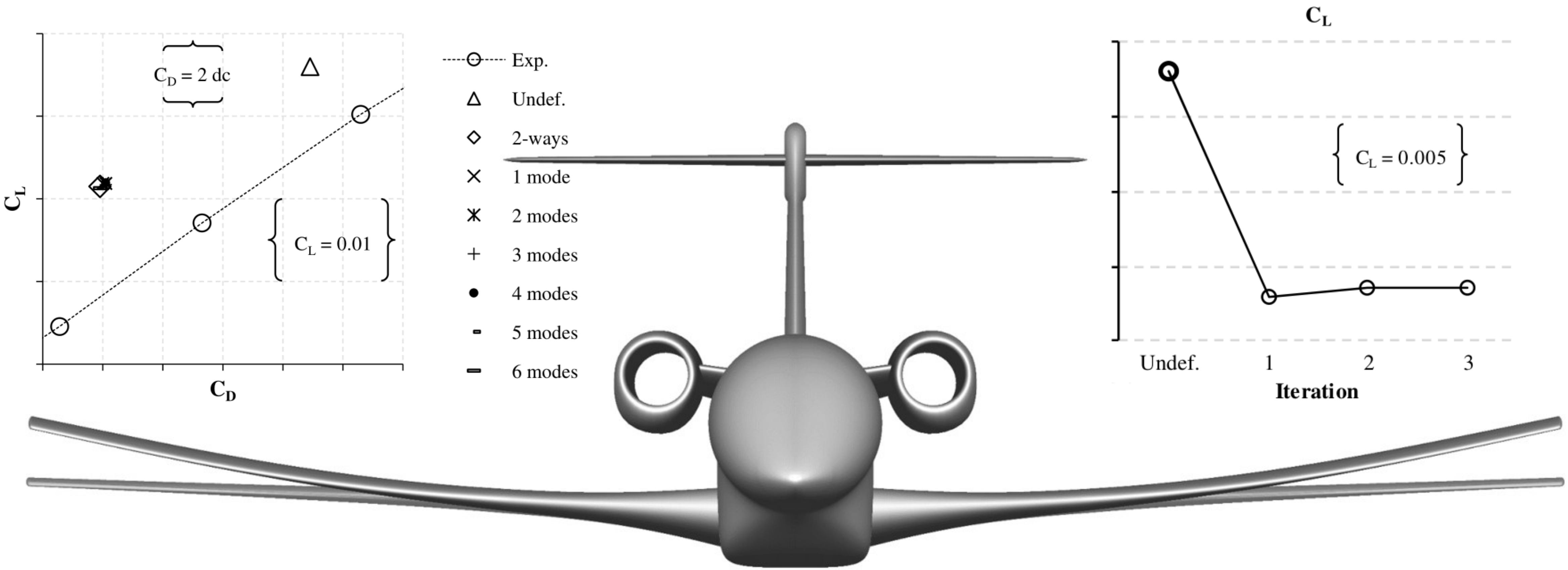

HIRENASD

- available on the database of the 1st NASA Aeroelastic Prediction Workshop (AePW)

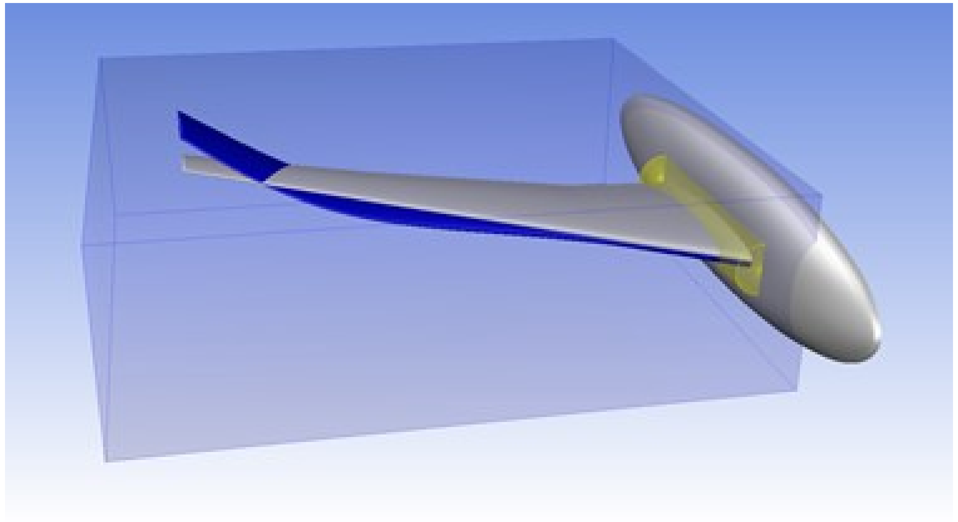

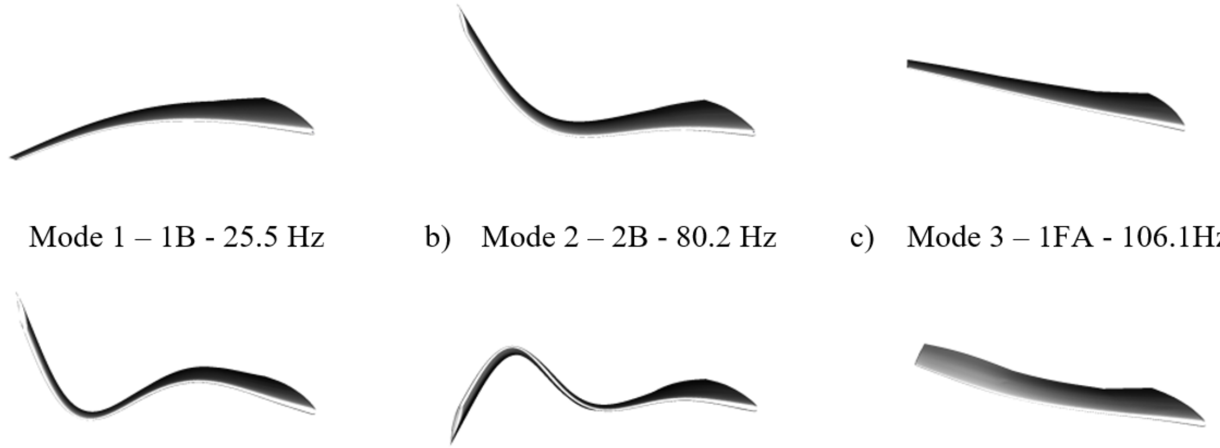

a) Mode 1 – 1B - 25.5 Hz
b) Mode 2 – 2B - 80.2 Hz
c) Mode 3 – 1FA - 106.1Hz
d) Mode 4 – 3B - 160.3 Hz
e) Mode 5 – 4B - 241.9 Hz
f) Mode 6 – 2FA - 252.2 Hz

HIRENASD

- Convergence reached in 3 FSI iterations

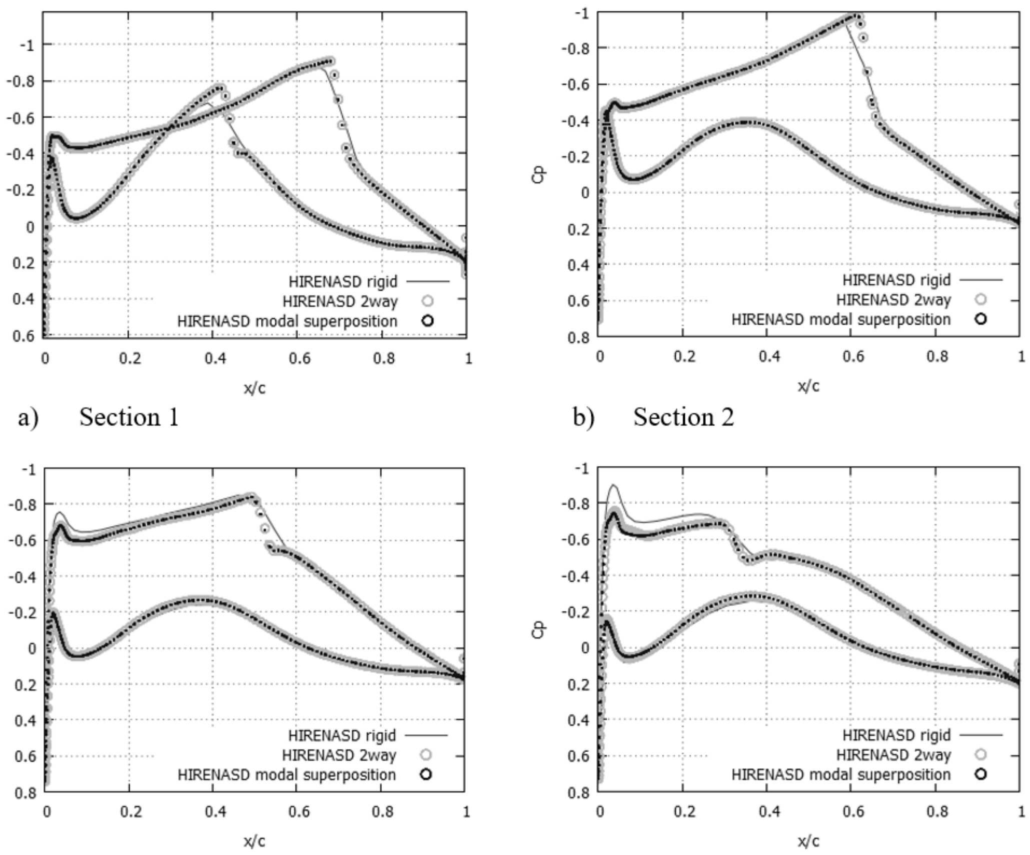

a) Section 1 b) Section 2

c) Section 5 d) Section 7

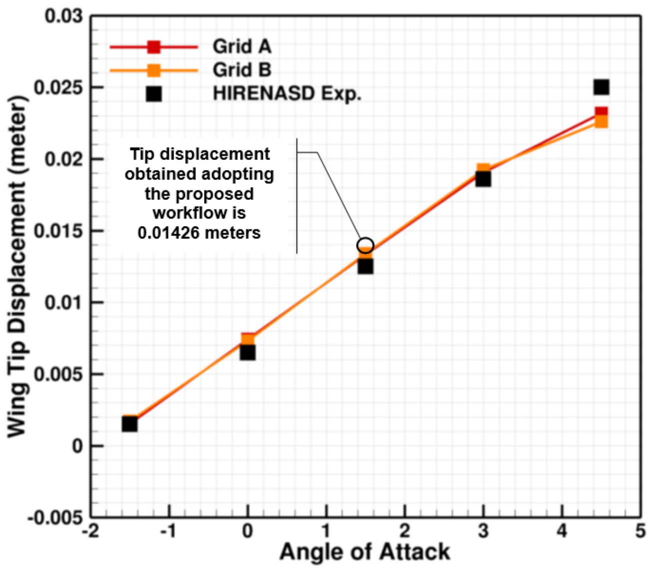

	Tip displacement (mm)	Relative discrepancy (%)
2-way	14.44	-
1 mode	15.26	-5.64
2 modes	14.18	1.81
3 modes	14.18	1.80
4 modes	14.26	1.29
5 modes	14.26	1.29
6 modes	14.26	1.29

RIBES wing

- FP7 European project, http://ribes-project.eu/

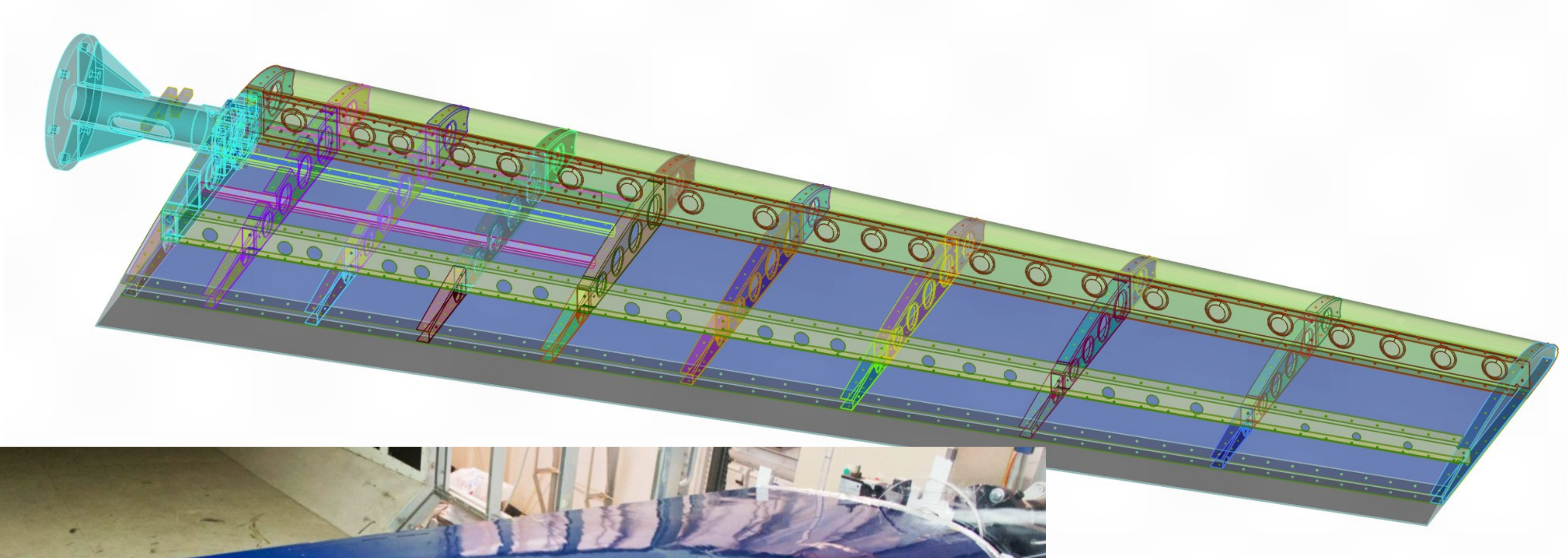

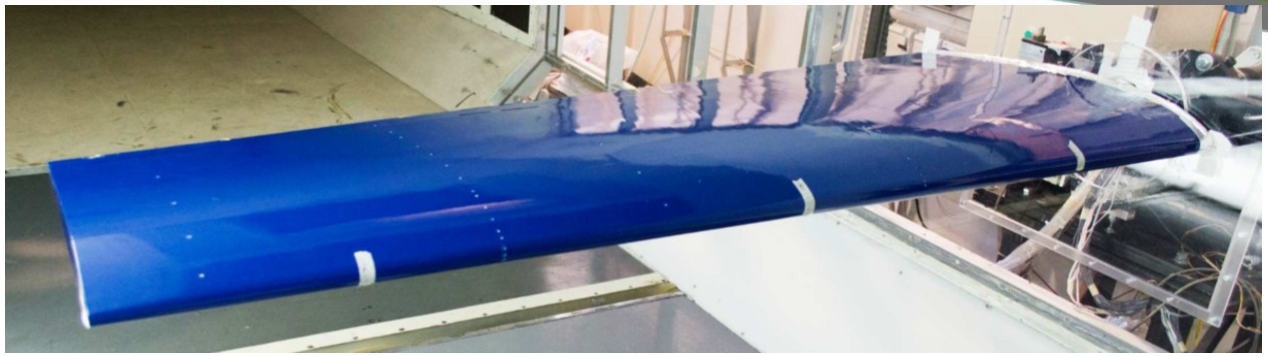

RIBES wing

- FP7 European project, http://ribes-project.eu/

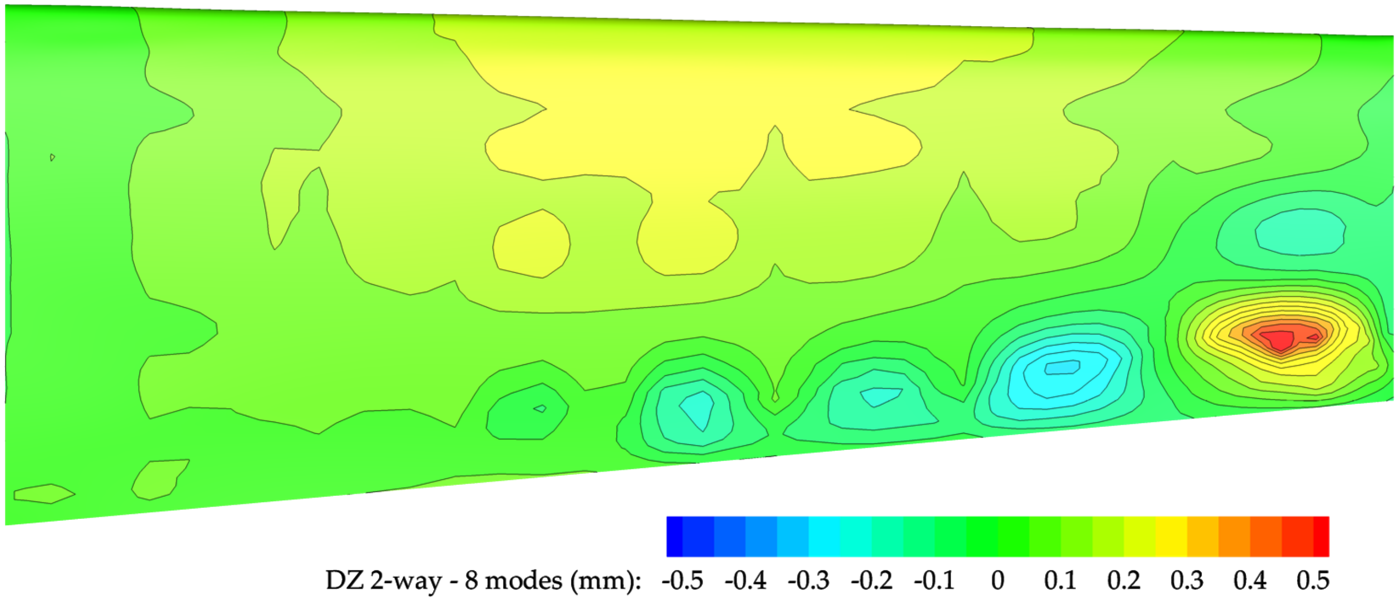

R I B E S

RBF4AERO-Fortissimo, Experiment 906

- Piaggio Aerospace Avanti EVO within the EU FORTISSIMO 2 project, using RBF4AERO platform

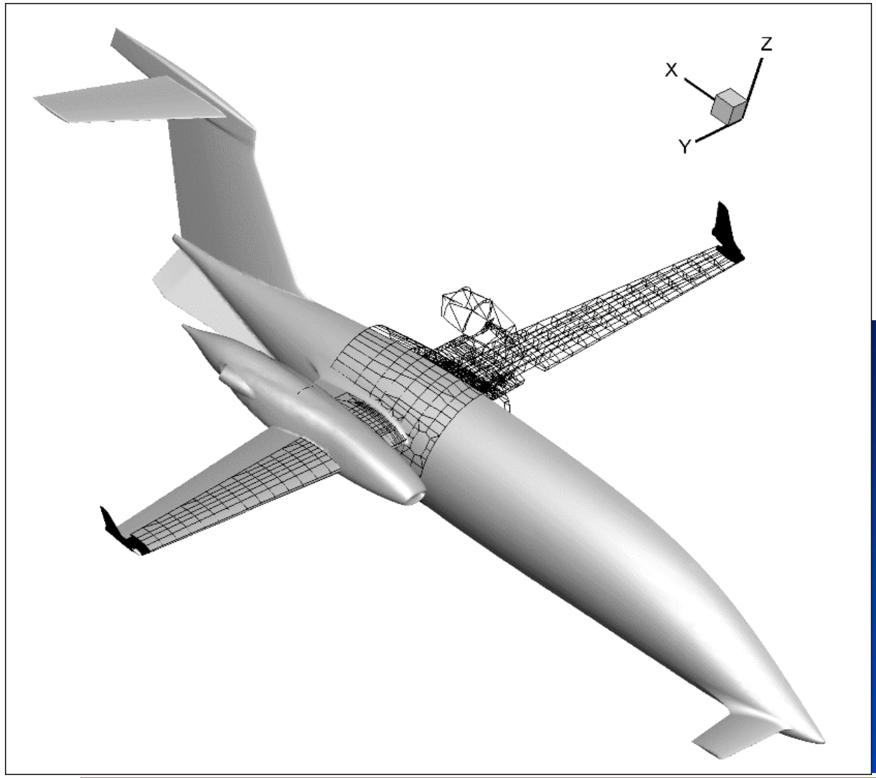

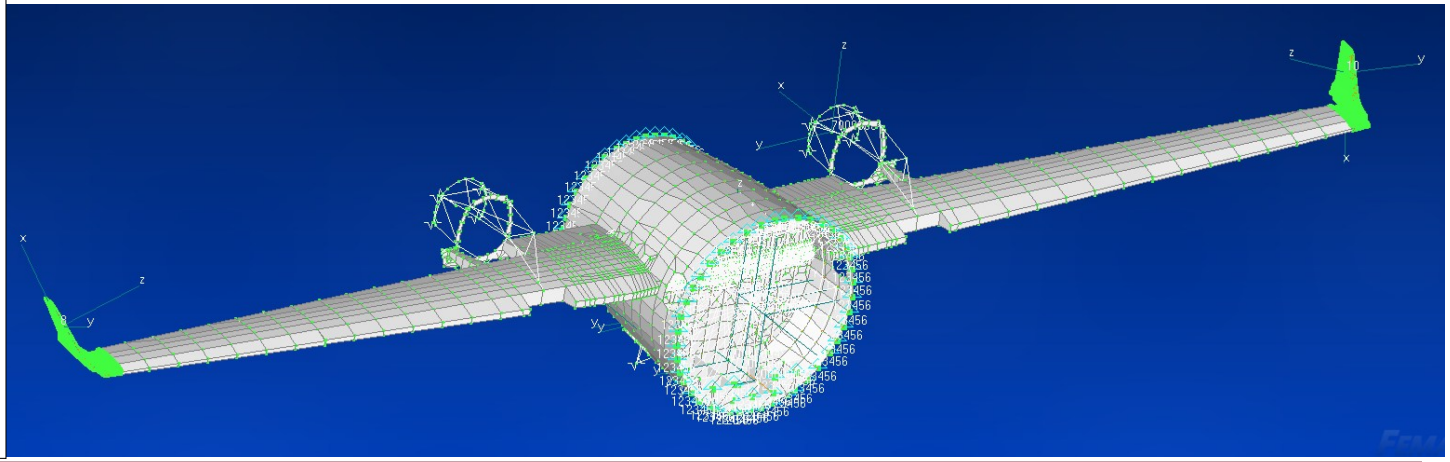

RBF4AERO-Fortissimo 2

- Non-matching CFD-CSM geometries, winglet twist, cant and sweep as shape parameters

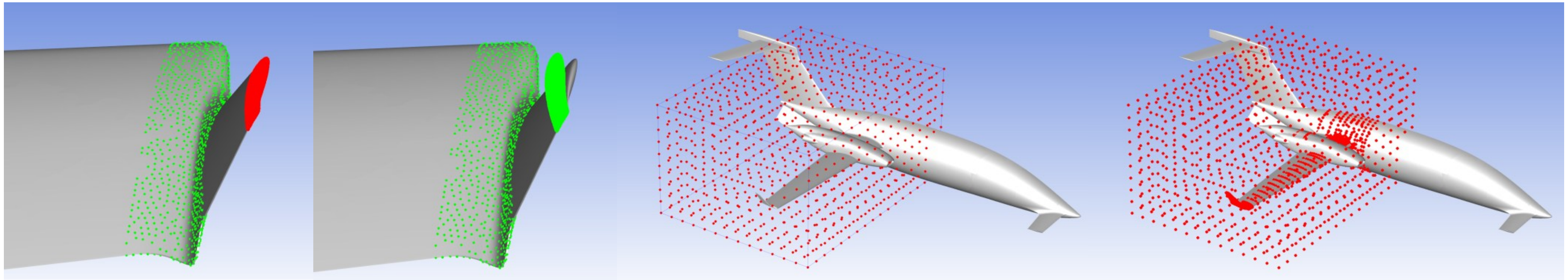

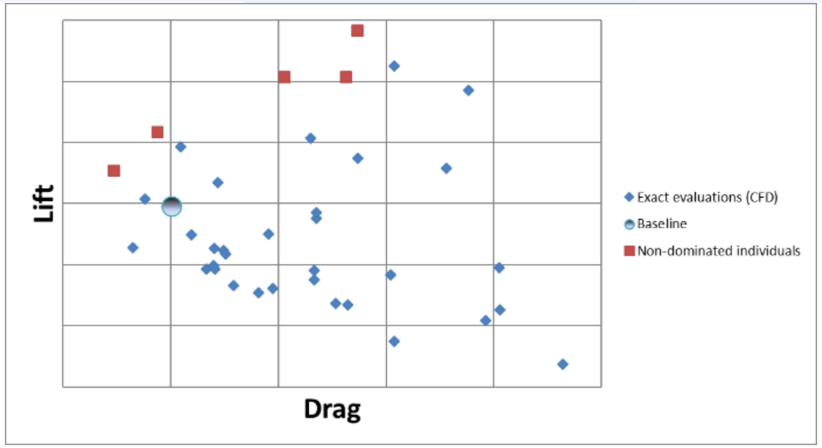

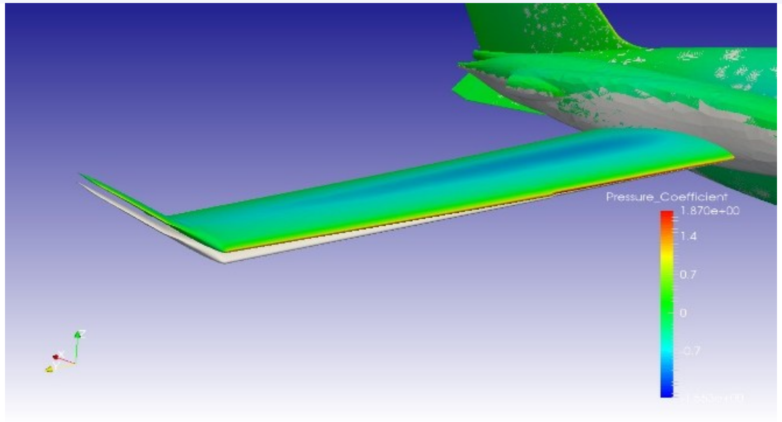

P180 Avanti EVO aircraft

Accurate Mapping in Fluid-Structure Interaction Analysis Across Models of Varying Fidelity Levels

Corrado Groth, Ubaldo Cella, Andrea Chiappa, Emiliano Costa, Giorgio Travostino, and Marco E. Biancolini

Abstract This paper addresses the aero-structural shape optimization of aircraft wings by integrating high-fidelity aerodynamic models that incorporate structural flexibility. We present a fluid-structure interaction (FSI) workflow designed for non-matching Computational Fluid Dynamics (CFD) and Computational Structural Mechanics (CSM) meshes, utilizing structural modes and Radial Basis Functions (RBF) for mesh morphing. The developed methodology is applied to an industrial case study: the winglet of the Piaggio Aerospace P180 Avanti EVO aircraft. The workflow successfully couples a hybrid Finite Element Analysis (FEA) model, which combines solid and lower-dimensional elements to represent the wing assembly (beam elements for the nacelle, shell elements for the wing box and solid elements for the winglet), with a high-fidelity CFD model.

Keywords FSI · Mode superposition · Mapping · Varying fidelity

P180 Avanti EVO aircraft

Fig. 4 Piaggio P180 Avanti EVO ©PiaggioAerospace

P180 Avanti EVO aircraft

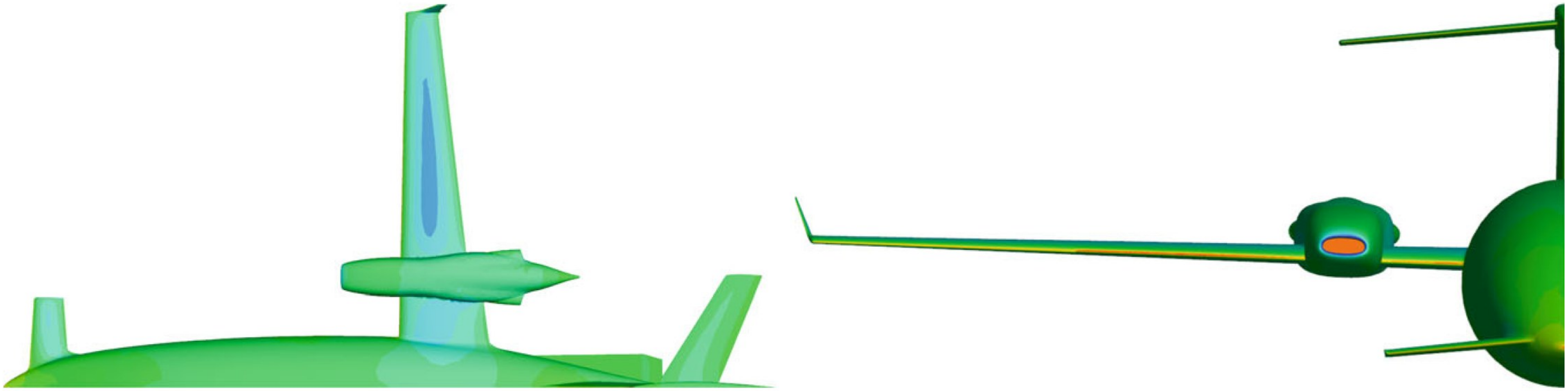

Fig. 5 C_p results obtained for the baseline configuration of the P180 model

P180 Avanti EVO aircraft

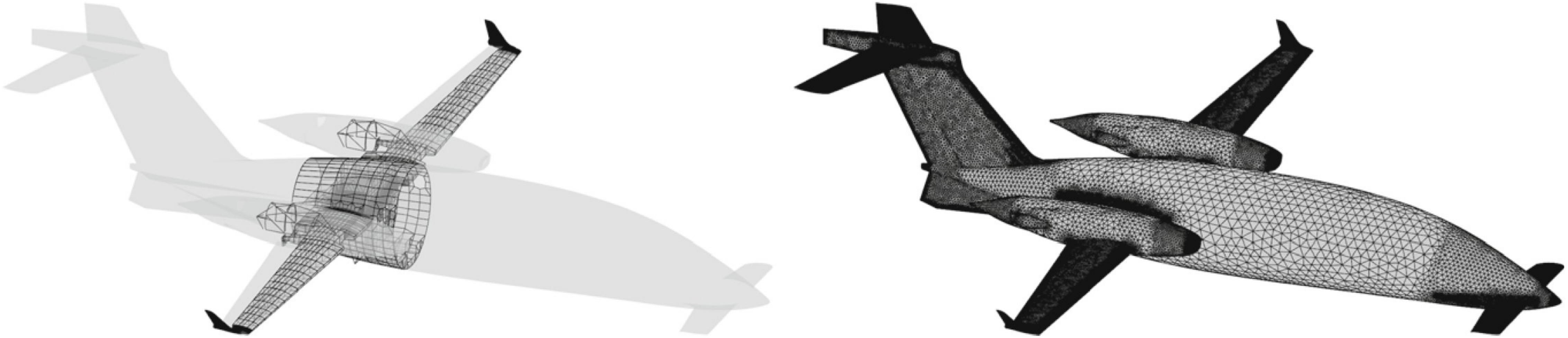

Fig. 6 Left: Piaggio P180 structural model employed for FSI computation, right: CFD model

P180 Avanti EVO aircraft

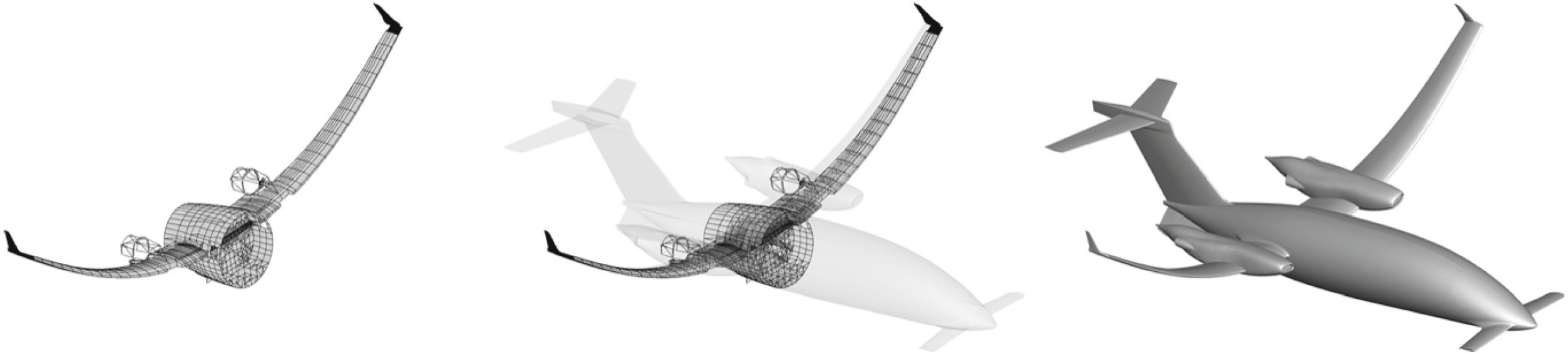

Fig. 7 First structural modal shape and transfer to the CFD mesh

P180 Avanti EVO aircraft

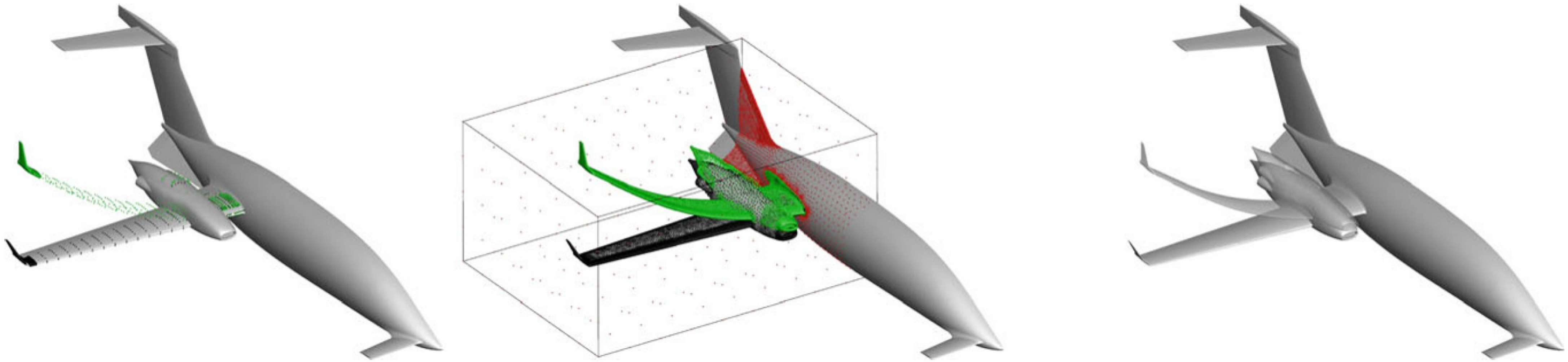

Fig. 8 RBF problem setup for the first modal shape. Left: RBF problem with FEM points, center: problem with fixed and moving sets, right: resulting CFD deformation

P180 Avanti EVO aircraft

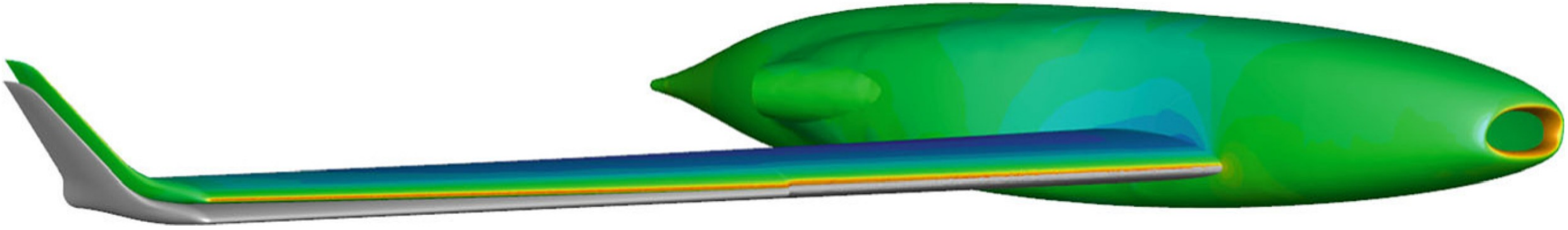

Fig. 9 Rigid–flexible model comparison for the baseline configuration

Coming soon...

Aerodynamic Optimization of an Aircraft Winglet Using **Ansys RBF Morph Fluids**

Conclusions

- An advanced workflow for FSI has been introduced
- The proposed FSI approach allows to quickly account of the structural deformration on the aerodynamic performances
- The past study about Piaggio P180 EVO is here used as an example showing how we can combine
  - FSI evaluated perfomances
  - Winglet design optimisation
- Work in progress on a different aircraft, more details will be added in the final publication

THANK YOU!

Marco Evangelos Biancolini

University of Rome Tor Vergata

biancolini@ing.uniroma2.it
https://www.linkedin.com/in/marcobiancolini/